IEC
Institute of Electronics and Computer

Journal of Artificial Intelligence and Systems, 2023, 5, 58-78
https://iecscience.org/journals/AIS
ISSN Online: 2642-2859

Trajectories modelling of mesoscale anticyclonic eddies in the Mozambique Channel using ANFIS Fuzzy C-Means

Hanitra Elisa Rasoavololoniaina[1, a, *], Harimino Andriamalala Rajaonarisoa[1, b], Todihasina Roselin Randrianantenaina[1, c], Adolphe Andriamanga Ratiarison[1, d]

[1]Laboratory of Atmosphere, Climate and Ocean Dynamics, University of Antananarivo, Science and Technology, Antananarivo, Madagascar
Email: [a.]hanitra.research@gmail.com; [b.]hariminondriamalala@gmail.com; [c.]todyroselin@yahoo.fr; [d.]adolphe.ratiarison.univ-antananarivo.mg@gmail.com
*Corresponding Author: Hanitra Elisa Rasoavololoniaina, Email: hanitra.research@gmail.com

How to cite this paper: Hanitra Elisa Rasoavololoniaina, Harimino Andriamalala Rajaonarisoa, Todihasina Roselin Randrianantenaina, Adolphe Andriamanga Ratiarison (2023). Trajectories modelling of mesoscale anticyclonic eddies in the Mozambique Channel using ANFIS Fuzzy C-Means. Journal of Artificial Intelligence and Systems, 5, 58–78. https://doi.org/10.33969/AIS.2023050105.

Received: May 8, 2023
Accepted: May 31, 2023
Published: June 5, 2023

Abstract

The aim of this paper is to optimize the Fuzzy C-Means (FCM) model of the ANFIS neuro-fuzzy system to model the four types of mesoscale anticyclonic eddy trajectories in the Mozambique Channel as a function of the variables eddy speed average of contour, amplitude and diameter, horizontal wind, atmospheric pressure and bathymetry. The study area concerns the eastern part of the Mozambique Channel between longitudes 41°E-44°E and latitudes 16°S-25°S. We classified the eddy trajectories of interest in our study area into four types according to their formation and dissipation zones. The data used are from the mesoscale eddy track atlas product derived from the META3 altimetry version. 1exp DT allsat for trajectories and eddy properties (amplitude, eddy rotation speed and diameter), GEBCO_2022 grid data for bathymetry, ECMWF data at spatial resolution 1° x 1° for atmospheric pressure, and Copernicus Marine data at spatial resolution 0.25° x 0.25° for wind. The latitudes and longitudes of the daily eddy displacement points from their formation to their dissipation characterize the trajectories. We used two different approaches in our study. The first approach consist to put each endogenous variable as input for the FCM model, while the second approach utilized the endogenous variables multiplied by the multiple regression coefficients. The results conclude that the case where the input variables of the model are preprocessed by the multiple (linear or polynomial) regression operation before FCM modeling is the best approach.

Keywords

Neuro-fuzzy modelling, mesoscale anticyclonic eddy, Mozambique Channel, ANFIS, Fuzzy C-Means, multiple regression

1. Introduction

Mesoscale oceanic eddies are elementary natural phenomena that play an important role in the movement of oceanic water masses [1]. They have an approximately circular structure and are found throughout the ocean [2]. Depending on the direction of the flow field rotation within the eddies, they are cyclonic or anticyclonic. In the Southern Hemisphere, if the direction is counterclockwise (respectively clockwise), the nature of eddy is cyclonic (respectively anticyclonic). In the northern hemisphere, the nomenclature is the opposite [3] [4]. Mesoscale oceanic eddies account for 90% of the kinetic energy of the oceans, which dominate the upper ocean flow field [5]. They generate significant impacts on large-scale oceanic circulations, and thus on the mass transport and biogeochemical properties of the ocean [5] and on the global energy cycle [6] [7]. Mesoscale coherent oceanic eddies (lifetimes greater than or equal to 30 days) capture nearly 80% of the total kinetic energy in the ocean [8]. The Mozambique Channel, an arm of the sea separating Madagascar from the African continent, contributes to the global redistribution of mass, heat, fresh water and other properties [9]. This channel, seat of an intense mesoscale eddy activity (100-300 km in diameter) [10], is known as a natural laboratory for the study of mesoscale oceanic eddies [11]. A study by Han Guoqing et al. (in 2019) shows oceanic anticyclonic eddies are far outnumber cyclonic inside the Mozambique Channel regardless of their lifetimes [12]. Studying lifetime eddies (greater than or equal to 30 days) ensures that mesoscale eddies are not a structures associated with synoptic-scale variability (days to a month).

Another peculiarity of Mozambique Channel is that it is a mines and gas geostrategic maritime transport zone, and rich in fishery resources. It represents 30% of the international oil trade and more than 5,000 ships move through it each year [13]. In terms of maritime accidents, recently in 2018, a cargo ship sank off the west coast of Madagascar that caused 8,000 liters of fuel oil to be spilled off the coast of this island [14] and caused oil pollution in the marine environment. Such an event may cause both physical (congestion, habitat suffocation) and toxic (contamination of organisms by chemical processes) impacts on aquatic fauna and flora. Several maritime disasters in the Mozambique Channel have resulted in physical damage and/or loss of life. . In 2015, the sinking of a dhow in Morondava, which is a common type of accident in the area, caused at least 28 deaths [15]; as well as the sinking of a boat in Majunga (in western Madagascar) in 2016, which resulted in 5 deaths, 13 survivors and missing [16].

The study of anticyclonic eddies trajectory is essential for activities monitoring at sea such as the navigation of dhows, the transport of oil, the offshore exploitation

that can cause oil spills, and the preservation of fishery resources.

Mesoscale oceanic eddies occur much more in the thin layers of the oceans than at depth and can be created by several mechanisms [17]. Thus, the environmental variables used for modelling are horizontal wind, pressure, and eddies properties such as rotation speed, diameter and amplitude. These properties are associated with each eddy and vary along its path. Wind is the first responsible for the movement of surface water [17]. Bathymetry is the underwater equivalent of terrestrial topography, and its influence on ocean eddies has been asserted by numerous studies [1]. By geostrophic equilibrium associated with the earth rotation, pressure is related to the Coriolis force [2].

The problem that arises is: how to model the trajectory of mesoscale anticyclonic eddies in the central eastern part of the Mozambique Channel from endogenous variables: speed average contour, amplitude and diameter of the eddy, as well as bathymetry, horizontal wind, atmospheric pressure, and latitude (respectively longitude)? Several approaches are able modelling this. In this work, we will use ANFIS-FCM model. In the following, we will discuss two approaches: the first one consists in taking each endogenous variable as input of ANFIS-FCM model. The second one uses the endogenous variables multiplied by the multiple regression coefficients as input variables of ANFIS-FCM model.

2. Methods

2.1. Study area

The study area is located between longitudes 41°E-44°E and latitudes 16°S-25°S. Figure 1 shows this area in a rectangular zone. This zone includes a maritime (blue), coastal (white) and terrestrial (brown) area, but we are only interested in the first two areas. On this figure, we also have the isobaths lines in continuous black except for the 1000m isobaths in red. The shallow (respectively deep) seawater is in light blue (respectively dark blue).

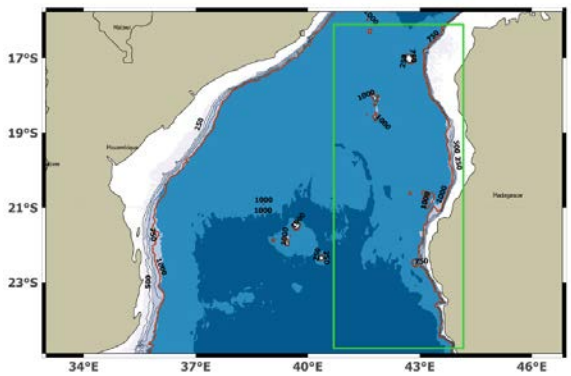

Figure 1. Study area, indicated by the green frame, with central Mozambique Channel topography and their continental shelf. The numbers of the isobaths inferior or equal to 1000m are displayed.

2.2. Data

2.2.1. Eddies trajectory and properties

The trajectory data and eddy properties are from the altimetry-derived mesoscale eddy trajectory atlas product META3.1exp DT[1] allsat version [18]. The data set includes daily information on anticyclonic and Cyclonic eddies detected from the multimission altimetry datasets, with their location, contours, amplitude, radius speed and associated metadata, for the whole altimetry period: January 1993-March 2020. The data are in classic NetCDF-4 format with CF standards.

Amplitude in [m] is the difference between the extremum of sea surface height (SSH) within the eddy and the SSH around the effective contour defining the eddy edge. Speed radius in (m) is the radius in of the best fit circle corresponding to the contour of maximum circum-average speed. Speed average in (m/s) is the average speed of the contour defining the radius scale "speed radius". Diameter in (Km) is the speed radius multiplied by 2 x 10^3.

From these daily data, we select the trajectories of length greater than or equal to 30 days and diameter between 100 Km and 300 Km. Then, we extract the daily properties of the eddies meeting these criteria. Then, we classify the trajectories according to the location of the longitudes and latitudes of each trajectory beginning and end with respect to the study area. Thus, we have four types of trajectory with their properties at each displacement (latitude and longitude) of eddies. Finally, we take a trajectory for each type, represented by the latitudes and longitudes of their daily displacement with their properties, in text format.

The length of the mesoscale anticylonic eddies trajectory for modelling varies from 43 to 256 days. Thus, Table 1 summarize the starting and ending latitudes and longitudes of the four trajectories for modelling.

Table 1. Start-End position and length of the four mesoscale anticyclonic eddies trajectory types

Trajectory	Starting latitude (°) and longitude(°)	Ending latitude (°) and longitude (°)	Length (day)
Type 1	-19.6; 43.48	-19.88 ; 41.92	43
Type 2	-19.32; 43.44	-22.55 ; 35.93	191

[1] The altimetric Mesoscale Eddy Trajectories Atlas product (META3.1exp DT allsat, DOI: 10.24400/527896/a01-2021.001) was produced by SSALTO/DUACS and distributed by AVISO+ (https://www.aviso.altimetry.fr/) with support from CNES, in collaboration with IMEDEA

Trajectory	Starting latitude (°) and longitude(°)	Ending latitude (°) and longitude (°)	Length (day)
Type 3	-13.33; 42.1	-16.3 ; 41.63	48
Type 4	-11.48; 44.37	-28.77 ; 33.78	256

2.2.2 Bathymetry

The bathymetric dataset2 used in our study is based on the GEBCO_2022 grid published in June 2022 in GeoTiff formats with files including the dataset documentation. It is a global terrain model for the ocean and land, providing elevation data, in meters, on a 15 arc second grid interval. With the global bathymetry data, we overlay the daily position data (latitude and longitude) along the four path types for modelling. Thus, we extract the bathymetries at each daily trajectory displacement.

2.2.3 Atmospheric pressure

Pressure data in Pascale units (Pa) is from the ECMWF reanalysis data in grid point and netcdf format available at https://charts.ecmwf.int/. We are interested in data between latitudes 11°S-29°S and longitudes 31°E-46°E. The data are at spatial resolution 1° x 1° for the period 1979 to 2018 and at regular intervals of four observations made every six hours (0000TU, 0600TU, 1200TU and 1800TU). We averaged these data to get the daily data. We then group the daily data according to the three parts of the Mozambique Channel (north, center and south) and make the spatial average. Thus, we have the daily spatial average at each division of the channel, which we then overlay with the daily position data along the four types of trajectory for modelling.

2.2.4 Horizontal wind at the sea surface

Wind data is Copernicus Marine reanalysis data in grid point and netcdf format [19]. These data are at 0.25° x 0.25° spatial resolution and daily time step for the period 1993 to 2019. We are interested in data between latitudes 11°S-29°S and longitudes 31°E-46°E. Then, we group these data according to the division (north, center and south) of the Mozambique Channel and we made the spatial average. Thus, we have the daily spatial average at each division of the channel, which we then overlay with the daily position data along the four types of trajectory for modeling.

2.3. Classification of eddies for the study area

In our study, we classify eddies trajectory into four types according to eddy

[2] GEBCO compilation group (2022) GEBCO_2022 grid (DOI: 10.5285/e0f0bb80-ab44-2739-e053-6c86abc0289c).

formation and dissipation locations. In this approach:

- Type 1 trajectory eddies are the eddies that born and dissipate in our study area;
- Type 2 trajectory eddies are the eddies that form in the study area and dissipate outside this area;
- Type 3 trajectory eddies are the eddies that born outside the study area and dissipate in this area;
- Type 4 trajectory eddies are the eddies that form and dissipate outside this area.

Thus, figures 2-a, 2-b, 2-c and 2d show the four categories of mesoscale anticyclonic eddy trajectories for modelling after classification.

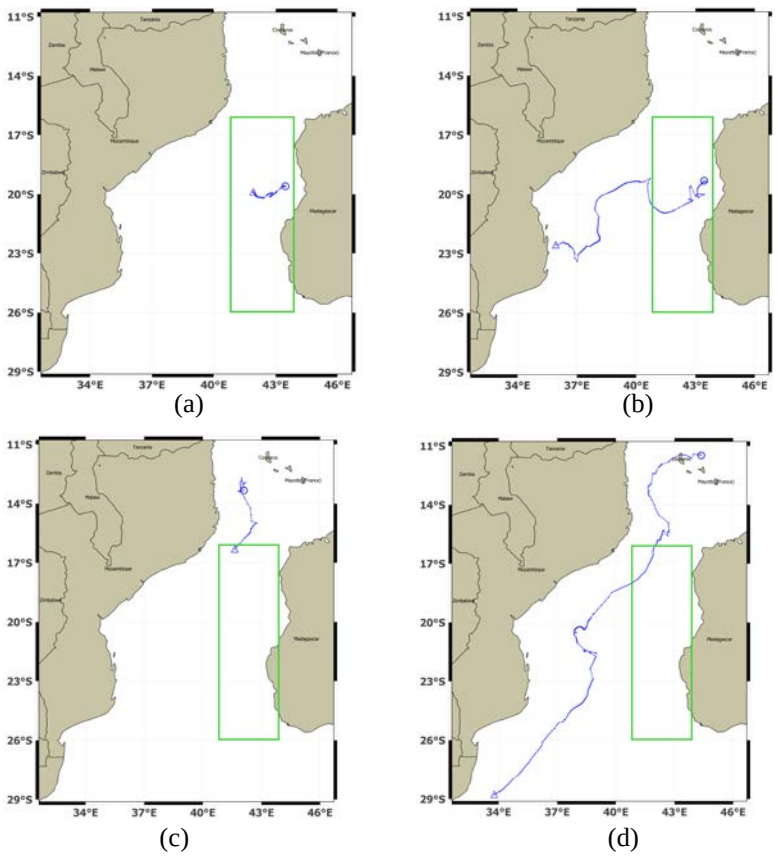

Figure 2. Illustration of the 4 trajectory types for modelling: (a) TYPE 1, (b) TYPE 2, (c) TYPE 3 and (d) TYPE 4. Round and triangle indicate respectively eddy formation and dissipation.

Table 2 shows endogenous variables obtained after data preprocessing.

Table 2. Endogenous variables used to model the four types of trajectories

Trajectory		Endogenous variables
Type 1	Latitude	Longitude; eddy speed radius, amplitude and diameter; bathymetry; pressure, wind speed and direction at Mozambique channel center.
	Longitude	Latitude; eddy speed radius, amplitude and diameter; bathymetry; pressure, wind speed and direction at Mozambique channel center.
Type 2	Latitude	Longitude; eddy speed contour, amplitude and diameter; bathymetry; pressure, wind speed and direction at center of Mozambique channel.
	Longitude	Latitude; eddy speed contour, amplitude and diameter; bathymetry; pressure, wind speed and direction at center of Mozambique channel.
Type 3	Latitude	Longitude; eddy speed contour, amplitude and diameter; bathymetry; pressure, wind speed and direction at north and center of Mozambique channel.
	Longitude	Latitude; eddy speed contour, amplitude and diameter; bathymetry; pressure, wind speed and direction at north and center of Mozambique channel.
Type 4	Latitude	Longitude; eddy speed contour, amplitude and diameter; bathymetry; pressure, wind speed and direction at north, south and center of Mozambique channel.
	Longitude	Latitude; eddy speed contour, amplitude and diameter; bathymetry; pressure, wind speed and direction at north, south and center of Mozambique channel.

2.4. Methodology adopted

Our method consists of two approaches. The first approach is that each endogenous variable rotational speed radius, amplitude and eddy diameter, latitude or longitude, bathymetry, wind, pressure is input of FCM model. The other approach is that the input variables of FCM model are the endogenous variables multiplied by the multiple regression coefficients (linear or polynomial). Latitude and longitude modelling are done separately but with the same procedures. For the second approach, if the coefficient of determination R^2 is less than 0.9, we use polynomial regression. In this case, we take one by one independently the endogenous variables in the model. The best model selected is the one with the highest coefficient of determination. Figure 3 shows the flowchart of the approach adopted.

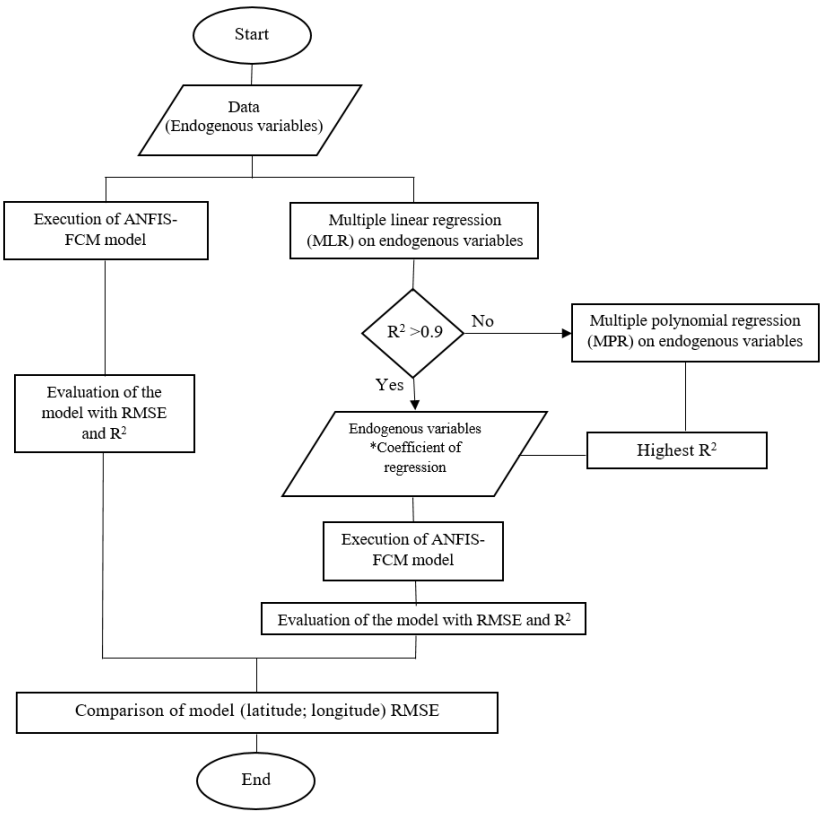

Figure 3. Flowchart of the approach adopted for ANFIS-FCM modelling

2.5. Multiple regression

Suppose that Y is the predicted variable (latitude or longitude) and X_1, X_2,..., X_p endogenous variables.

Equation (1) is the equation of multiple linear regression:

$$Y = b_0 + b_1 \times X_1 + b_2 \times X_2 + ... + b_p \times X_p + \xi \quad (1)$$

b_0: Constant corresponding to Y value when all values of X_1, X_2,..., X_p are zero;

b_1, b_2,..., b_p : unknown coefficients of the model;

Y: vector representing the dependent variable;

X_1, X_2,..., X_p : vectors representing the different endogenous variables;

ξ : white noise.

Equation (2) is the equation of multiple linear regression:

$$Y = a_1 X^1 + a_2 X^2 + ... + a_n X^n + \xi \quad (2)$$

$a_1, a_2, ..., a_p$: unknown coefficients of the model;

X: endogenous variable;

ξ : white noise.

2.6. Adaptive neuro-fuzzy inference system (ANFIS) and Fuzzy C-Means (FCM)

The adaptive neuro-fuzzy inference system (ANFIS), presented by Jang in 1993, is a hybrid multilayer model [20] [21]. ANFIS is built by combining fuzzy inference and artificial neural networks to complement the disadvantages of each method [22]. The modeling approach is derived from a Takagi Sugeno type fuzzy inference system that composed of antecedents and consequents [23] [24]. Basic ANFIS network architecture uses 5 layers neural network as shown in Figure 4.
The content and operation of each layer is defined as follows:

- Layer 1 is responsible for collecting and preprocessing input data to make it suitable for training ANFIS network. Each neuron in this layer is associated with a specific input variable and passes the input data to the neurons in the next layer;

- Layer 2 represents the fuzzy membership functions (MF) of the input variables. It uses fuzzy mathematical functions to model the fuzzy relationships between input values and the degrees of membership in different fuzzy categories. We use the generalized Gaussian function for our case;

- Layer 3 expresses the fuzzy logic rules that relate the membership values of the input variables' fuzzy functions to the membership value of the output variable's fuzzy function. It uses neurons to represent the different fuzzy rules as IF-THEN conditions, where the antecedents (respectively consequents) are the membership values of the input (respectively output) of fuzzy functions;

- Layer 4 aggregates the outputs of the neurons in the rule layer to obtain an overall estimate of the output value. It combines the membership values of the output variable fuzzy functions using T-norm or S-norm operations to obtain a single aggregated membership value;

- Layer 5 generates the final output of the ANFIS network by combining the aggregate membership value of the output variable into a global fuzzy membership function. This global fuzzy membership function is used to compute the final output value using appropriate defuzzification operations to obtain a

final numerical value or decision.

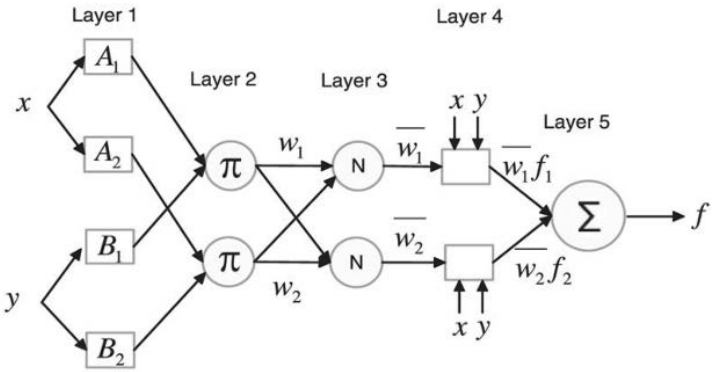

Figure 4. ANFIS model architecture (Zhang et al. 2010)

The clustering method is fundamental when modelling with ANFIS [25]. FCM is one of the three clustering techniques proposed by ANFIS to organize data into comparable fuzzy clusters [23]. This technique is based on a fuzzy set and least square method by improving the k-means clustering technique proposed by Bezdek [26] [27]. ANFIS uses backpropagation gradient descent in this least square method to optimize FCM model parameters.

Figure 5 shows the architecture of ANFIS model with FCM clustering method [28]. It's resume of the following steps:

Step 1: random selection of each cluster centers c_j , j=1,2,…,c from the n data patterns $\{X_1, X_2, X_3, ..., X_n\}$;

Step 2: calculation of the membership matrix with equation (3):

$$u_{ij} = \frac{1}{\sum_{k=1}^{c} \left(\frac{\|X_i - c_j\|}{\|X_i - c_k\|} \right)^{\frac{2}{m-1}}}, \quad m > 1 \tag{3}$$

Where u_{ij} is the degree of membership of object i to cluster j, m is the weighting exponent, X_i is the i-th of the measured d-dimensional data, c is the number of clusters, and c_j the cluster center [29]

Step 3: Calculation of the objective function with the equation (4) and iteratively optimization of the function by updating the membership u_{ij} of the data in group j;

$$E = \sum_{i=1}^{N}\sum_{k=0}^{n} u_{ij}^{m} \left\| x_i - c_j \right\|^2, 1 \le m \le \infty \tag{4}$$

The process stops when $\max_{ij}\left\{u_{ij}^{(k+1)} - u_{ij}^{(k)}\right\} < \varepsilon$

ε is the user-defined stopping criteria.

Step 4: Calculation of new cluster center c_j, j=1,2,…,c with the equation (5):

$$c_j = \frac{\sum_{i=1}^{N} u_{ij}^{m} . x_j}{\sum_{i=1}^{N} u_{ij}^{m}} \tag{5}$$

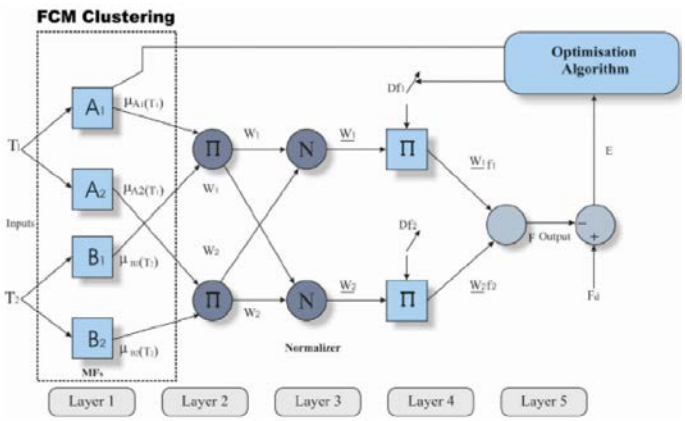

Figure 5. Basic structure of ANFIS with FCM clustering method [28]

Unlike k-means where each observation could be linked to one and only one cluster, FCM allows data points to belong to multiple clusters [30]. The dominant cluster for each data point is determined by the probability of its proximity that is between 0 and 1 [22]. In ANFIS-FCM model, the input data can be variables or features from different domains, and the output can be a class or a continuous value.

ANFIS model gives very good results in trajectory tracking and nonlinear approximation [24] and ANFIS-FCM method is applicable to a wide variety of problems of the geostatistical data analysis.

For our case, we use it in the modeling context. As input we have the endogenous variables (detailed in Table II) indicated by X_1, X_2,...,X_p in Figure 6, or the endogenous variables multiplied by their multiple regression coefficients (linear or

polynomial) indicated by $b_1X_1+b_2X_{2+}...+b_pX_p$ in Figure 7 for linear regression, and by $a_1X^1+a_2X^2{}_+...+a_pX^p$ in Figure 8 for polynomial regression. As output, we have the latitude or longitude indicated by Y. Thus, the mappings of ANFIS-FCM model inputs and outputs represented by figures 6, 7 and 8 change according to the adapted approach as explained in section 2.3. Indeed, figure 6 illustres the first approach and the second one, which differs according to the inputs of the model, is represented by figure 7 (with multiple linear regression) and figure 8 (with polynomial regression).

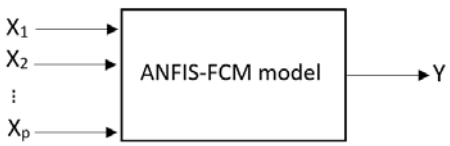

Figure 6. Mapping of ANFIS-FCM model inputs and outputs for the first modeling approach.

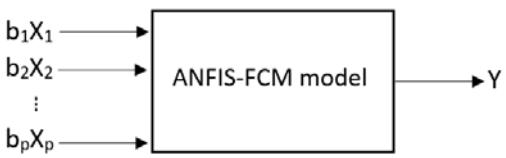

Figure 7. Mapping of ANFIS-FCM model inputs and outputs for the second modeling approach using multiple linear regression.

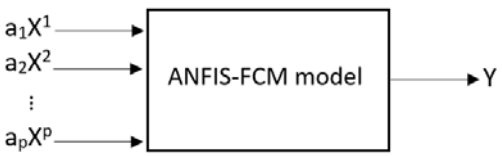

Figure 8. Mapping of ANFIS-FCM model inputs and outputs for the second modeling approach using polynomial regression.

Following Figure 9 summarizes the approach we use to apply the ANFIS-FCM model:

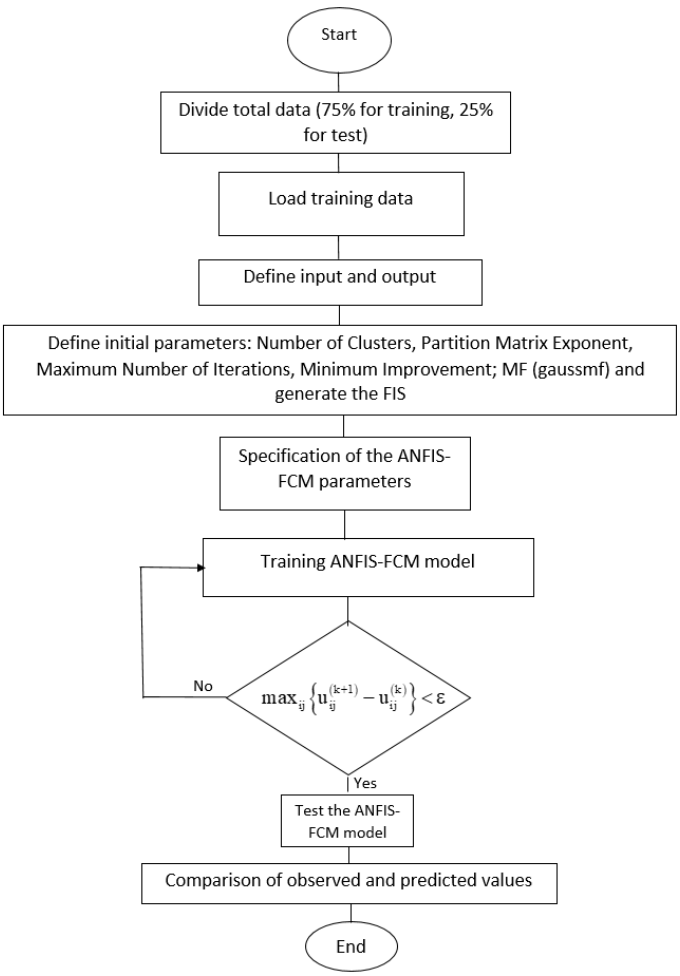

Figure 9. Flowchart of ANFIS-FCM modeling [29]

2.7. Evaluation of model performance

In this study, two statistical indices were used as evaluation criteria: the root mean square error (RMSE) and the coefficient of determination (R^2).

2.7.1. Root mean square error

Following equation (6) gives the expression of the RMSE error:

$$RMSE = \sqrt{\frac{1}{N}\sum_{t-1}^{N}(y_t - \hat{y}_t)^2} \quad (6)$$

y_t and $\hat{y}_t$ are respectively the observed and predicted values and N the number of

observations.

2.7.2. Coefficient of determination R^2

The coefficient of determination R^2 measures the geometric fit of the model to the data [31] [32] Following equation (7) defines this relation:

$$R^2 = corr\left(\hat{y}_i, y_i\right)^2 = 1 - \frac{\sum_{i=1}^{n}\left(y_i - \hat{y}_i\right)^2}{\sum_{i=1}^{n}\left(y_i - \bar{y}_i\right)^2} \quad (7)$$

Where n is the number of observations, y_i the value of measure number i, $\hat{y}_i$ the corresponding predicted value and $\bar{y}_i$ the mean of the measures.

$R^2 \in [0; 1]$ Interpretation of limit cases [31].

3. Results

3.1. Results of ANFIS-FCM models using both approaches

We performed approximately 30 model parameterization attempts with 75% training data and 25% test data. Table 3 shows the results of modeling the longitudes and latitudes of the four trajectory types with the ANFIS-FCM model using both approaches. We can see that the second one represents the best R^2 determination coefficients whatever the trajectory type modeled.

Table 3. Experimental results of ANFIS-FCM models using both approaches

Model output	Modeling approach	Number of clusters	Exponential partition matrix	Maximum number of iterations	Initial step size	RMSE train	RMSE test	R^2 test
Trajectory TYPE 1								
Latitude	2nd	15	4	100	0.1	$1.36*10^{-4}$	$2,2*10^{-2}$	$99,63*10^{-2}$
	1st	15	4	100	0.1	$3.18*10^{-3}$	0.1	$83,14*10^{-2}$
Longitude	2nd	15	2	20	0.8	$3.46*10^{-5}$	$6,3*10^{-2}$	$99,19*10^{-2}$
	1st	15	2	20	0.1	$0.93*10^{-3}$	2,17	$12,9*10^{-2}$

Trajectory TYPE 2								
Latitude	2nd	5	3	3	0.8	$7*10^{-3}$	0,14	$99,42*10^{-2}$
	1st	5	3	3	0.8	$7.6*10^{-2}$	$1,6*10^{-2}$	$99,2*10^{-2}$
Longitude	2nd	8	2	200	0.1	$6.3*10^{-3}$	$14,6*10^{-2}$	$99,8*10^{-2}$
	1st	8	2	200	0.1	0.2	$66,6*10^{-2}$	$97,06*10^{-2}$
Trajectory TYPE 3								
Latitude	2nd	6	4	5	0.1	$6.2*10^{-6}$	$27,9*10^{-2}$	$99,36*10^{-2}$
	1st	6	4	5	0.1	$2.3*10^{-3}$	35,1	$18,05*10^{-2}$
Longitude	2nd	5	2	50	0.01	$1.9*10^{-4}$	$7,3*10^{-2}$	$91,93*10^{-2}$
	1st	5	2	50	0.01	$8.5*10^{-3}$	9,5	$22,58*10^{-2}$
Trajectory TYPE 4								
Latitude	2nd	15	10	5	0.6	$1,3*10^{-2}$	0,4	$99,73*10^{-2}$
	1st	15	10	5	0.6	$3,4*10^{-2}$	1,7	$95,09*10^{-2}$
Longitude	2nd	15	10	20	0.6	$2,1*10^{-3}$	0,15	$99,85*10^{-2}$
	1st	15	10	20	0.6	$1,5*10^{-2}$	1,7	$85,8*10^{-2}$

3.2. Graphical representations of the best models for the four trajectory types

Figures 10-a, 10-b, 10-c, 10-d illustrate the best models of the four trajectory types, combining longitudes and latitudes, whose characteristics are given by Table 3. The longitudes are on the x-axis and the latitudes on the y-axis. On each figure, the red and blue curves represent respectively the observation and the model. Both curves have the same shape. For these best models, the second approach is the most suitable for our case. We show in figure 11 the approach established for the best model (case of the TYPE 1 trajectory model: RMSE $=1.13 \times 10^{-2}$).

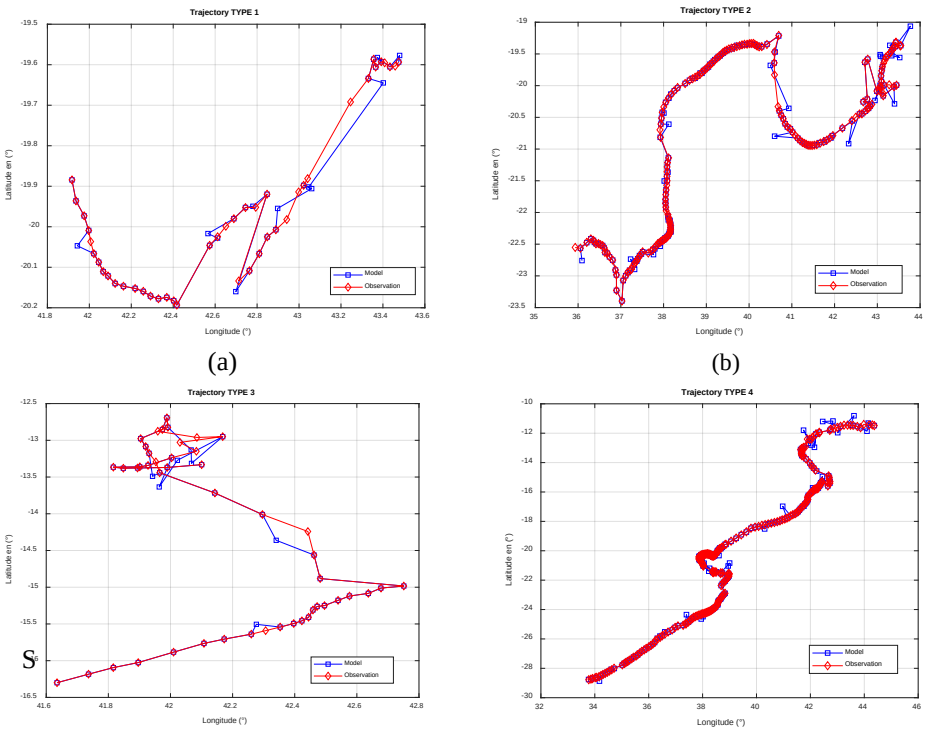

Figure 10. Model of the four trajectory types of mesoscale anticyclonic eddy in the Mozambique Channel: (a)-TYPE 1, (b)-TYPE 2, (c)-TYPE 3 and (d)-TYPE 4.

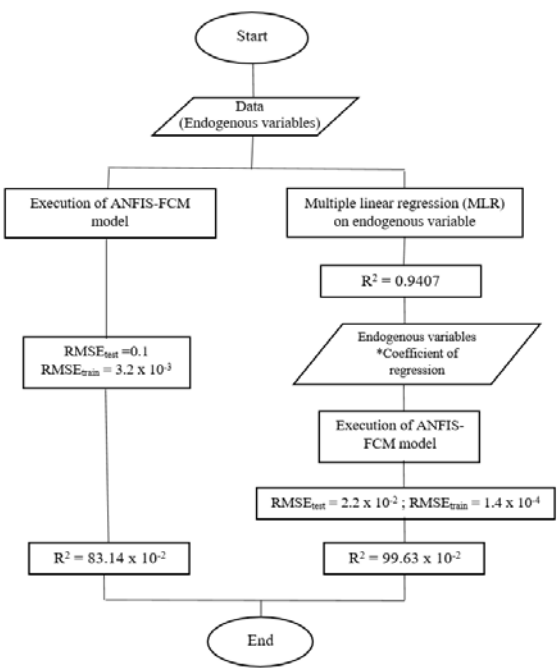

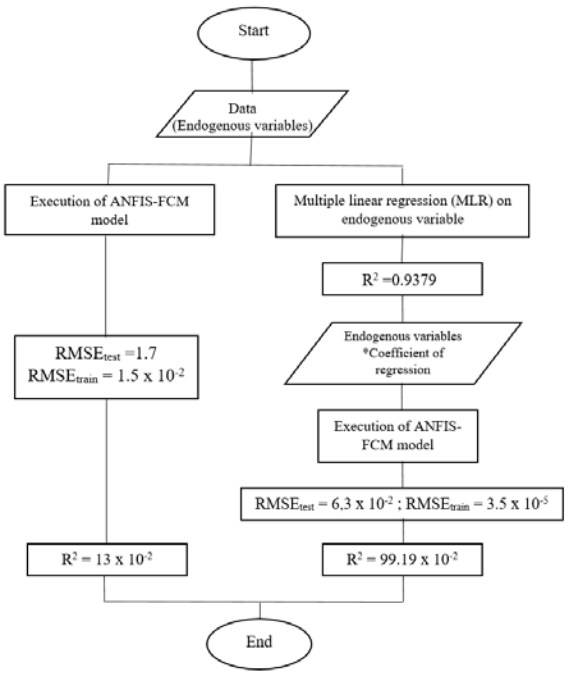

Figure 11. TYPE 1 trajectory modeling approach: (a)-latitude, (b)-longitude

4. Discussion

ANFIS-FCM method is widely used in various application domains such as meteorology (to model complex and dynamic data), industrial processes, finance, etc... [28] [33] [34]. Kim and al. used this method to classify 855 typhoons tracks, between 1965-2006 period in the Pacific Northwest into seven groups. The seven groups are characterized by typhoons striking, affecting, passing, crossing or moving directly over some cities in their study area [33]. S. Gokten et al. also applied the method on financial health scoring applies the FCM algorithm to produce unique and sensitive financial scores. Their results show that the calculated scores are consistent with short-term price formations in terms of investor behavior and that the FCM clustering algorithm could be used to sort companies from a more sensitive perspective [34]. We use this technique to model the trajectories of mesoscale oceanic eddy. We first classify the trajectories of mesoscale anticyclonic eddies relevant to our study area. This method consists of classifying these eddy trajectories into four types, according to their place of formation and dissipation. T. Zhang et al. also used a mesoscale ocean eddy classification method to classify the mesoscale eddies in the North China Sea shelf into four types. Their approach

consist to classify the mesoscale eddies according to their motion paths: along-the-isobath type, intrusion-of-continental-shelf type, local wandering type, and shelf-internal-generation type [35]. Both approaches are used in the same application domain but with different objectives. In their case, the aim is to perform a statistical analysis of the eddies, whereas for us the objective is to model the trajectories of interest in our study area.

After this classification, we apply the FCM model with each type of trajectory obtained using the two approaches mentioned in section 2.3. The limitation of our method is that we have to stop at 2 degree polynomial in the second approach because of the large number of input variables and the limit related to the computer performance.

4. Conclusion

In conclusion, we applied the ANFIS-FCM method using two approaches to model the four types of mesoscale anticyclonic eddy trajectories of interest in the eastern part of the central Mozambique Channel. The first approach is to use each endogenous variable characterizing the eddy displacements as input of FCM model. The second approach consists in multiplying the endogenous variables by the coefficients of multiple regression (linear or polynomial) before to put as inputs of FCM model. The endogenous variables used are speed contour, amplitude and eddy diameter, latitude or longitude, bathymetry, horizontal wind (speed and/or direction) and atmospheric pressure. In the second approach, the coefficients of determination R^2 are better than in the first approach for the four types of trajectory. The model also uses the RMSE to evaluate the difference between the observed and predicted trajectory (characterized by latitude and longitude). Thus, the RMSE for each type of trajectory are 1.13×10^{-2} for type 1; 5.53×10^{-2} for type 2; 10.76×10^{-2} for type 3 and 15.13×10^{-2} for type 4. The models obtained are excellent because they all have an RMSE close to 0.

The originality of our work is the application of the ANFIS-FCM method in the modeling of mesoscale oceanic eddy trajectories. Our study revealed that the modeling results are better by pre-treating the endogenous variables with multiple regression before putting them as input to the ANFIS-FCM model.

References

[1] TEINTURIER, S. (2008) Dynamique et stabilité de tourbillons océaniques en interaction avec la côte et la topographie, in ENS / Polytechnique - Laboratoire de Météorologie Dynamique *École Nationale Supérieure de Techniques Avancées* p. 210.

[2] AGUEDJOU, H.M.A. (2022) Caractéristiques des tourbillons de mésoéchelle dans locéan Atlantique tropical et leurs interactions avec latmosphère., in

SDU2E - Sciences de l'Univers, de l'Environnement et de l'Espace *Université d'Abomey-Calavi (UAC), BENIN-Cotutelle internationale Université Toulouse 3 - Paul Sabatier*.

[3] Zhang, Z., et al. (2013) Universal structure of mesoscale eddies in the ocean. Geophysical Research Letters. 40. https://doi.org/10.1002/grl.50736

[4] Zhang, Z., W. Wang, and B. Qiu. (2014) Oceanic mass transport by mesoscale eddies. Science. 345(6194): p. 322-324. https://doi.org/10.1126/science.1252418

[5] Zhang, Z., et al. (2022) Coherence of Eddy Kinetic Energy Variation during Eddy Life Span to Low-Frequency Ageostrophic Energy. Remote Sensing. 14(15): p. 3793. https://doi.org/10.3390/rs14020379

[6] Aiki, H., X. Zhai, and R. Greatbatch. (2015) *ENERGETICS OF THE GLOBAL OCEAN: THE ROLE OF MESOSCALE EDDIES*. https://doi.org/10.1142/9789814696623_0004

[7] Chen, R., G.R. Flierl, and C. Wunsch. (2014) A Description of Local and Nonlocal Eddy–Mean Flow Interaction in a Global Eddy-Permitting State Estimate. Journal of Physical Oceanography. 44(9): p. 2336-2352. https://doi.org/10.1175/JPO-D-14-0009.1

[8] Richardson, P.L. (1983) Eddy kinetic energy in the North Atlantic from surface drifters. *Journal of Geophysical Research*: Oceans. 88(C7): p. 4355-4367. https://doi.org/10.1029/JC088iC07p04355

[9] Dimarco, S., et al. (2002) Volume transport and property distribution of the Mozambique Channel. Deep Sea Research Part II: Topical Studies in Oceanography. 49: p. 1481-1511. https://doi.org/10.1016/S0967-0645(01)00159-X

[10] Tew Kai, E. (2009) Rôle des tourbillons méso-échelle dans la structuration spatiale de l'écosystème pélagique : le cas du canal de Mozambique Role of mesoscale eddies in the spatial structuring of the pelagic ecosystem: Case of the Mozambique Channel.

[11] Twekai, E. and F. Marsac. (2010) Tourbillons méso-échelle et top prédateurs dans le canal de Mozambique. Information spatiale pour l'environnement et les territoires. 9: p. 44.

[12] Han, G., et al. (2019) SST Anomalies in the Mozambique Channel Using Remote Sensing and Numerical Modeling Data. Remote Sensing. 11(9): p. 1112. https://doi.org/10.3390/rs11091112

[13] Tristan COLOMA, Q.R.F.Y. (2022) Le canal du Mozambique : un espace de compétition crisogène.

[14] LINFO. (2018) Canal du Mozambique : un cargo sombre avec 8 000 litres de fuel au large de Madagascar, in LINFO.RE.

[15] LINFO. (2014) Belo sur Tsiribihina : le naufrage d'un boutre fait trois morts, in LINFO.RE.

[16] LINFO. (2015) Madagascar : 5 morts dans un naufrage d'une vedette à Majunga, in LINFO.RE.

[17] Roullet, G., et Patrice Klein. (2011) La turbulence océanique de méso-échelle, in *Le climat à découvert*, CNRS, Editor.

[18] AVISO. MESOSCALE EDDY TRAJECTORY ATLAS PRODUCT META3.1EXP DT. [cited 2020; Available from: https://www.aviso.altimetry.fr/en/data/products/value-added-products/global-mesoscale-eddy-trajectory-product/meta3-1-exp-dt.html.

[19] Marine, C. Global Ocean Physics Reanalysis. [cited 2020; Available from: https://data.marine.copernicus.eu/products.
[20] Jang, J.-S. (1993) ANFIS: adaptive-network-based fuzzy inference system. *IEEE transactions on systems, man, and cybernetics*. 23(3): p. 665-685. https://doi.org/10.1109/21.256541
[21] Esmaili, M., et al. (2021) Assessment of adaptive neuro-fuzzy inference system (ANFIS) to predict production and water productivity of lettuce in response to different light intensities and CO2 concentrations. Agricultural Water Management. 258: p. 107201.
[22] Yeom, C.-U. and K.-C. Kwak. (2018) Performance Comparison of ANFIS Models by Input Space Partitioning Methods. Symmetry. 10: p. 700. https://doi.org/10.3390/sym10120700
[23] Adedeji, P.A., et al. (2020) Wind turbine power output very short-term forecast: a comparative study of data clustering techniques in a PSO-ANFIS model. *Journal of Cleaner Production*. 254: p. 120135. https://doi.org/10.1016/j.jclepro.2020.120135
[24] Bezzini, A. (2008) Commande Prédictive Non Linéaire en Utilisant Les Systèmes Neuro-Flous et les Algorithmes Génétiques.
[25] Adedeji, P., N. Madushele, and S. Akinlabi. (2018) Adaptive Neuro-fuzzy Inference System (ANFIS) for a multi-campus institution energy consumption forecast in South Africa. in *Proceedings of the International Conference on Industrial Engineering and Operations Management Washington DC, USA, September 27-29 of Conference*.
[26] Bezdek, J. (1981) Pattern Recognition With Fuzzy Objective Function Algorithms. https://doi.org/10.1007/978-1-4757-0450-1
[27] Bezdek, J.C. (1973) FUZZY-MATHEMATICS IN PATTERN CLASSIFICATION. *Cornell University*.
[28] Abdulshahed, A., A. Longstaff, and S. Fletcher. (2014) Thermal error modelling of machine tools based on ANFIS with fuzzy c-means clustering using a thermal imaging camera. Applied Mathematical Modelling. https://doi.org/10.1016/j.apm.2014.10.016
[29] Oladipo, S., Y. Sun, and A. Amole. (2022) Performance Evaluation of the Impact of Clustering Methods and Parameters on Adaptive Neuro-Fuzzy Inference System Models for Electricity Consumption Prediction during COVID-19. Energies. 15(21): p. 7863.
[30] Abdulshahed, A.M., A.P. Longstaff, and S. Fletcher. (2015) The application of ANFIS prediction models for thermal error compensation on CNC machine tools. *Applied soft computing*. 27: p. 158-168. https://doi.org/10.1016/j.asoc.2014.11.012
[31] Laffly, D. (2006) Régression multiple : principes et exemples d'application. Available from: https://www.scribd.com/document/76603425/Laffly-Regression-Multiple.
[32] Cornillon, P.A. and E. Matzner-Lober. (2012) Régression avec R. *Springer Paris*. https://doi.org/10.1007/978-2-8178-0184-1
[33] Kim, H.-S., et al. (2011) Pattern Classification of Typhoon Tracks Using the Fuzzy c-Means Clustering Method. *Journal of Climate*. 24(2): p. 488-508. https://doi.org/10.1175/2010JCLI3751.1

[34] Gokten, S., P. Gokten, and F. Başer. (2017) Using fuzzy c-means clustering algorithm in financial health scoring. *Audit Financiar Journal*. 15: p. 385-394. https://doi.org/10.20869/AUDITF/2017/147/385

[35] Zhang, T., et al. (2022) Statistical Analysis of Mesoscale Eddies Entering the Continental Shelf of the Northern South China Sea. *Journal of Marine Science and Engineering*. 10(2): p. 206. https://doi.org/10.3390/jmse10020206